THE JOURNAL OF COMPARATIVE NEUROLOGY 430:343–356 (2001)

Distribution of S- and M-Cones in Normal and Experimentally Detached Cat Retina

KENNETH A. LINBERG,[1] GEOFFREY P. LEWIS,[1] CHUNGLING SHAAW,[1] TONIA S. REX,[1,2] AND STEVEN K. FISHER[1,2]*
[1]Neuroscience Research Institute, University of California, Santa Barbara, Santa Barbara, California 93106-5060
[2]MCD Biology, University of California, Santa Barbara, Santa Barbara, California 93106-9610

ABSTRACT

The lectin peanut agglutinin (PNA) and antibodies to short (S)- and medium to long wavelength (M/L)-sensitive cones were utilized in order to define the relative distributions of the two spectral types of cone across the domestic cat's retina. These values, in turn, were compared to those from retinas that had been experimentally detached from the retinal pigment epithelium. The pattern of cone distribution in the normal cat's retina is established by the preponderance of M-cones that constitute between 80% and 90% of all cones. Their peak density of over 26,000 cells/mm^2 resides at the *area centralis*. Though M-cone density decreases smoothly to the ora serrata where they have densities as low as 2,200 cells/mm^2, the density decrease along the nasotemporal axis is slower,creating a horizontal region of higher cone density. S-cones constitute between 10% and 20% of all cones, the number being quite variable even between individual animals of similar age. The highest S-cone densities are found in three distinct locations: at the superior far periphery near the ora serrata, immediately at the *area centralis* itself, and in a broad zone comprising the central and lower half of the inferior hemiretina. S-cones in the cat retina do not form a regular geometrical array at any eccentricity. As for the detached cat retina, the density of labeled S-cone outer segments (OS) decreases rapidly as early as 1 day postdetachment and continues decreasing to day 28 when the density of cones labeling with anti-S opsin has dropped to less than 10% of normal. This response points to a profound difference between rods and cones; essentially all rods, including those without OS, continue to express their opsin even in long-term detachments. The implications of these results for visual recovery after retinal reattachment are discussed. J. Comp. Neurol. 430:343–356, 2001.

Indexing terms: photoreceptors; blue cones; lectins; antibodies; retinal detachment

The cat's retina has long been used as a model approximating the human retina because it contains both rods and cones and has a central region of high cone density, the *area centralis*, which in many respects is similar to our own fovea. Steinberg et al. (1973) determined that unlike the human rod-free fovea (Østerberg, 1935), the cat's *area centralis*, though the site of highest cone density (25,000 to 30,000/mm^2), nonetheless is 90% rod-populated. The cat's rod-driven night vision is legendary; its capacity for color vision, controversial. Behavioral (Loop et al., 1987) and physiological studies (Daw and Pearlman, 1970; Cleland and Levick, 1974; Ringo et al., 1977; Weinrich and Zrenner, 1983), as well as analyses using electroretinography (Rabin et al., 1976; Zrenner and Gouras, 1979), have implicated two spectral subtypes of cone in the cat's vision and suggest that short wavelength-sensitive cones (S-cones) are far outnumbered by the medium to long wavelength-sensitive cones (M-cones). The present study was undertaken to describe the distribution of the S- and M-cones in the normal cat retina and to attempt to quan-

Grant sponsor: NIH; Grant number: EY00888.

*Correspondence to: Steven K. Fisher, Ph.D., Neuroscience Research Institute, University of California, Santa Barbara, Santa Barbara, CA 93106-5060. E-mail: fisher@lifesci.ucsb.edu

Received 13 March 2000; Revised 17 October 2000; Accepted 26 October 2000

tify the relative fates of the two types after experimental retinal detachment. It is presumably the loss of photoreceptors and/or their imperfect regeneration that accounts for the visual deficits often remaining after successful surgical repair of retinal detachments. Detachment results in a rapid onset of photoreceptor cell death and then a transition to a gradual though sustained loss of these cells (Erickson et al., 1983; Cook et al., 1995). Even in the long-term detachments, however, a variable population of both rods and cones survive albeit with a highly "degenerative" or "primitive" morphology (Erickson et al., 1983). It is not clear whether cones die at a different rate than rods, or whether S-cones are more susceptible to injury than the M-cones as has been reported in humans after retinal detachment (Nork et al., 1995). Portions of this report have appeared elsewhere in abstract form (Linberg et al., 1998).

MATERIALS AND METHODS

Fifteen domestic cats were used in this study; all were female between 7 and 9 months of age. Cats were entrained to a 12-hour light, 12-hour dark lighting schedule; their care was overseen by a resident veterinarian, and their experimental use was conducted in compliance with both the guidelines of the UCSB Animal Care Council and the *ARVO Statement for the Use of Animals in Ophthalmic and Vision Research.* Cats were euthanized with an overdose of sodium pentobarbitol (120 mg/ml).

Experimental retinal detachments

Large retinal detachments (50% to 75% of each retina) were created in the right eyes of domestic cats by infusing a solution of 0.25% sodium hyaluronate (Healon, Pharmacia, Kalamazoo, MI; in balanced salt solution; Alcon Labs; Ft. Worth, TX) via a glass micropipette between the retina and the retinal pigmented epithelium (RPE; for further details see Anderson et al., 1986). The small amount of Healon prevents the retinas from reattaching. The superior temporal quadrant containing the *area centralis* was always completely detached. The animals were killed at 1, 3, 7, and 28 days after detachment.

Tissue processing

Eyes were fixed in chilled 4% paraformaldehyde in 0.1 M sodium cacodylate buffer, pH 7.4. The eye cups first were divided into nasal and temporal halves by using the optic nerve head (ONH) as a landmark, then into quadrants by using the lower edge of the *tapetum lucidum* as a line of reference. Tissue was stored in this fixative at 4°C until wholemounts were reconstructed from these quadrants.

Lectin and immunocytochemical labeling

Neural retina was carefully peeled away from the RPE. The retinal quadrants were then rinsed in phosphate-buffered saline (PBS, pH 7.4), blocked for at least 2 hours in normal donkey serum (1:20), and labeled overnight at 4°C with either the biotinylated lectin, peanut agglutinin (PNA; 400 μg/ml; Vector Labs; Burlingame CA), or antibodies to rhodopsin (1:50; gift of Dr. R. Molday, University of British Columbia, Vancouver, Canada), M/L- (JH492) and S-cone (JH455) opsins (1:2,000; gifts of Dr. J. Nathans, The Johns Hopkins University Medical Center, Baltimore, MD), and calbindin D (1:1,000; Sigma; St. Louis, MO). After rinsing the wholemounts in a solution containing PBS, bovine serum albumin (0.5%), Triton X-100 (0.1%), and sodium azide (0.1%), they were placed overnight in this same solution containing various combinations of either streptavidin-cy3 (1:100; Jackson ImmunoResearch; West Grove, PA) or one of the secondary antibodies: goat-anti-rabbit fluorescein (1:50; Cappel; West Chester, PA), donkey-anti-rabbit or -mouse cy2, cy3, or cy5 (1:200; Jackson ImmunoResearch).

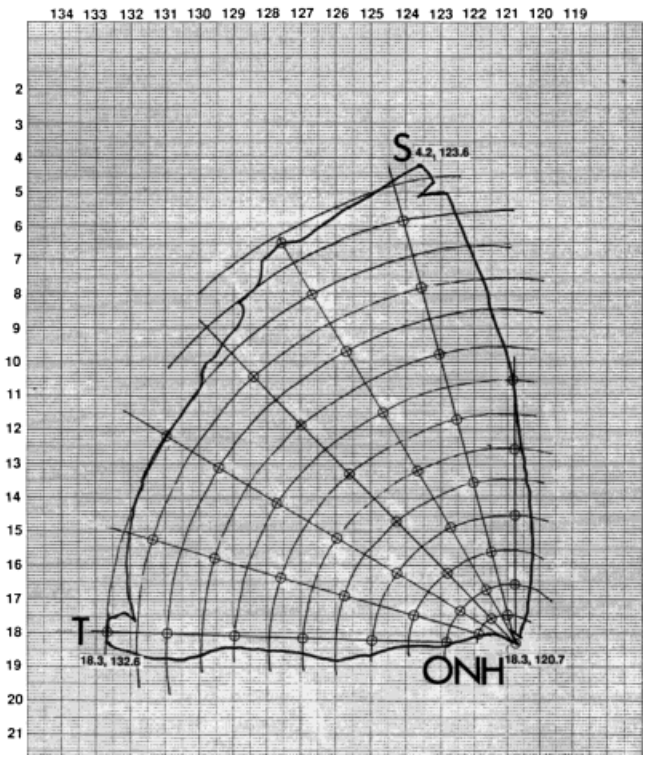

Fig. 1. Diagram showing how sampled areas of each retinal quadrant were selected for the quantitation of cone subtypes. Each circle represents a sampling area of about 0.2 mm^2. ONH, optic nerve head; S, superior; T, temporal.

Preparing wholemounts

Retinal quadrants were mounted photoreceptor side up onto microscope slides by using 5% n-propyl gallate in glycerol. Cover slips were sealed by using fingernail polish. Scaled drawings of each quadrant were superimposed on a grid whose coordinates corresponded to those on the micrometer stage settings of an Olympus BX60 System microscope. This allowed any retinal location to be recorded within 0.1 mm. The maps for each quadrant were divided into 15° sectors by using the ONH as their point of origin. Photographs were taken along the edges of these regions at 1-mm intervals, offset by 0.5 mm for every other edge (Fig. 1). Multiple, nonoverlapping regions were sampled near the *area centralis* of every specimen. Several of these sites were studied with a BioRad 1024 laser scanning confocal microscope. No corrections were made for possible shrinkage during the fixation or mounting of the wholemounts; the tissue was never dehydrated in any solvents and the quadrants were mounted by using the hydrophilic mounting medium, n-propyl gallate.

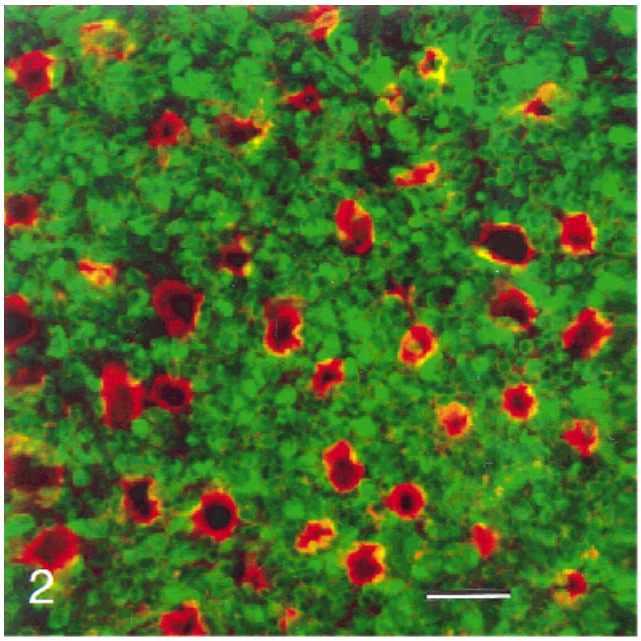

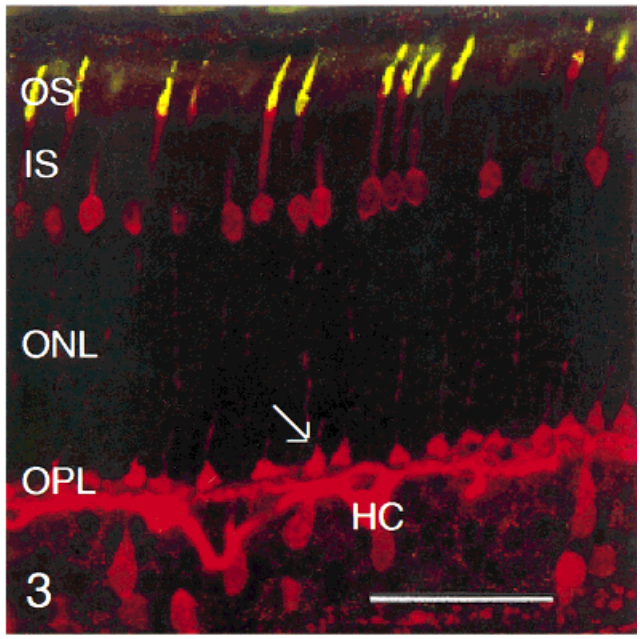

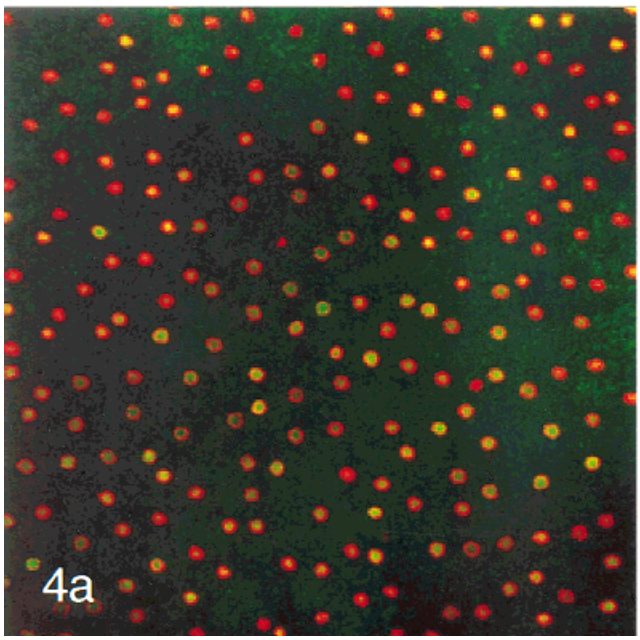

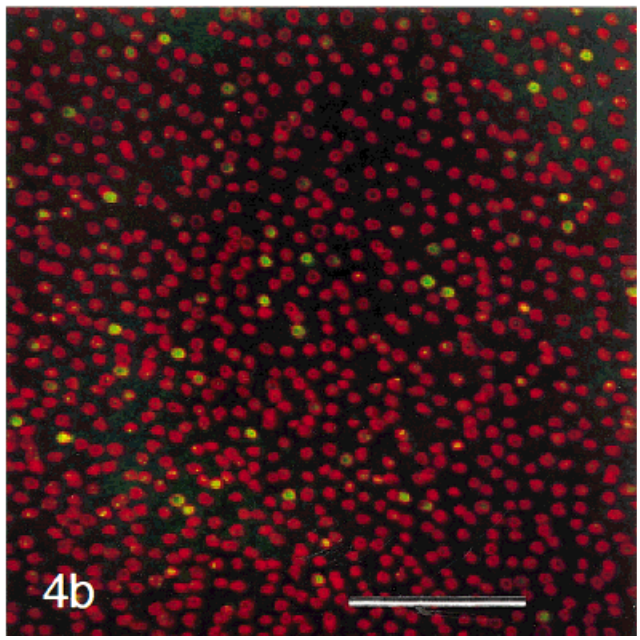

Fig. 2. Confocal micrograph of pericentral cat retina stained with the lectin peanut agglutinin (PNA; red) to label the matrix sheath around all cone outer segments (OS) (Johnson et al., 1986), and the antibody to rhodopsin (green) to label rod OS. Though there are small points of overlap (yellow) of the two antibodies seen at the top of the figure, this is likely an artifact of photoreceptor obliquity. We never observed any rod OS (green) surrounded by cone matrix sheaths (red). Scale bar = 10 μm.

Fig. 3. Confocal micrograph of a transverse section through the cat retina labeled with antibodies to calbindin D (red) and medium to long wavelength (M/L) opsin (green; yellow = colocalization). Calbindin D labels the whole cone photoreceptor from outer segments (OS) to the synaptic pedicle (arrow), but less intensely than the subjacent horizontal cells (HC). IS, inner segments; ONL, outer nuclear layer; OPL, outer plexiform layer. Scale bar = 50 μm.

Fig. 4. Wholemounted cat retina labeled with the lectin peanut agglutinin (PNA; red) and an antibody to calbindin D (green). **a:** In the midperiphery, all cone matrix sheaths (PNA) contain calbindin D-positive outer segments (OS). All peripheral cones are presumably calbindin D-positive. **b:** In the *area centralis*, most cones are calbindin D-negative. Scale bar = 50 μm.

Quantitation

At each of the selected retinal locations, pairs of fluorescent micrographs were taken by using a 20× objective lens: one of all cone sheaths in the field labeled with biotinylated PNA or all cone cells labeled with the monoclonal antibody to calbindin D (rhodamine channel), and the other of cone outer segments labeled by the antibody against S-cone opsin (fluorescein channel). Individual cones were counted manually. Counts were normalized to cones/mm^2 at their respective positions on the whole-

mounted quadrant. Isodensity contours were fitted to the data and coded by a gray scale such that regions of highest density were black with areas of decreasing density being increasingly lighter shades of gray. In order to limit the number of experimental animals, we did not repeat such counts by using wholemounts labeled with the antibody against M/L-opsin. In control animals, the relative density of M-cones at each retinal location sampled was derived from taking the difference between the densities of PNA-positive (i.e., all cones) and S opsin-positive profiles. Unfortunately, in the detached retinas, such a method could not be used (see below).

RESULTS

Normal cat retina

Labeling with PNA and antibodies against S-cone opsin and rhodopsin. In the normal cat retina, we used PNA to label the cone matrix sheaths around all cone types (Bridges, 1981; Blanks and Johnson, 1984; Johnson, Hageman and Blanks, 1986), and the JH455 antibody against S-cone opsin to specifically label S-cone outer segments (OS; Wang et al., 1992). Comparing paired micrographs of the same photoreceptor fields, the positions of labeled S-cone OS always corresponded to identifiable PNA-positive cone sheaths (for example, compare Fig. 7B, left, right). In order to be certain that we were not including a subpopulation of rod sheaths that might be PNA-positive, a phenomenon reported in 0.3% of rods in the human retina (Iwasaki et al., 1992), we double-labeled one retinal quadrant with PNA and anti-rhodopsin to screen for any co-localization (Fig. 2). We found no cone sheaths surrounding rod outer segments.

Quantitative analysis of cone distributions in the normal cat's retina. Wholemounted quadrants from two normal left eyes were labeled with anti-S opsin and the lectin PNA. Multiple sample areas of approximately 0.2 mm^2 each were selected as described above (Fig. 1) and photographed. Although these control retinas were from two young cats (one a week over 8 months, the other a week short of 8 months) of similar genetic background, there was variation in the data between the two eyes, and between respective quadrants. Such variations in photoreceptor populations are hardly novel. The data are summarized in Figure 5. We counted 195 sample areas in one eye ($\sim$ 39 mm^2) containing 252,006 cones, 16.4% of which were labeled with antibodies to S-cone opsin. A second normal eye was sampled at 180 sites ($\sim$ 36 mm^2) that collectively contained 226,784 PNA-positive cone sheaths, 12.9% of which corresponded to S opsin-positive OS (Fig. 5A). When broken down by quadrant (Fig. 5B), the two inferior quadrants of each eye showed elevated numbers of S-cones compared with their respective superior quadrants.

Figure 6 is a schematic representation of the total cone distribution in the wholemounted retina depicted on the left side of Figure 5. The regional variation in cone density is indicated (see gray scale at bottom left) by using isodensity contours derived from data taken at the 195 sampling sites (black dots). Peak cone density lies at the *area centralis* that is central to an elongated region of higher cone density along the nasotemporal axis, a morphological entity first described by Steinberg et al. (1973). The highest density we encountered in the *area centralis* of 27,483

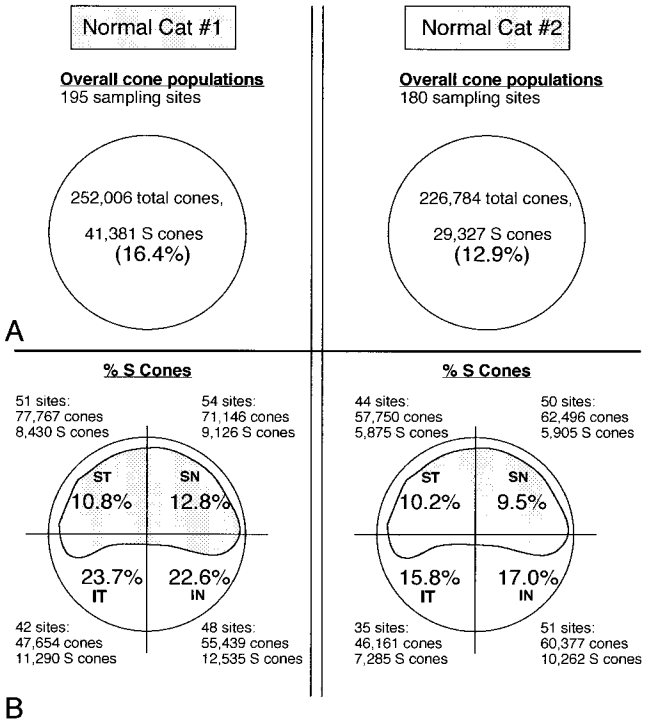

Fig. 5. The total number of cones counted manually in two normal cat retinas. **A:** Total number of labeled peanut agglutinin (PNA) sheaths versus short wavelength (S)-cones in cat #1 (left) and cat #2 (right). **B:** The same data broken down by quadrant and focusing on percent S-cones. The shaded region represents that portion of the cat's retina underlain by a pigment-free retinal pigmented epithelium (RPE) and the *tapetum lucidum*. Retinal quadrants: ST, superior temporal; SN, superior nasal; IT, inferior temporal; IN, inferior nasal.

cones/mm^2 falls well within the range of values they reported of 26,000 to 30,000/mm^2. Sampling sites containing fewer than 5,000/mm^2 are restricted to zones at the far periphery of all quadrants (the lowest density we measured was 3,105/mm^2). At each sample site, a pair of light micrographs was taken as described above; 8 of these are shown in Figures 7A to 7H and correspond to labeled positions (A–H) within Figure 6. All the micrographs of Figure 7 are shown at the same magnification (see scale bar in Fig. 7A): the left member of each pair shows PNA-positive cone sheaths representing the total number of cones in its field, whereas the right micrograph in each pair reveals those OS that are S opsin-positive. Not surprisingly, the diameter of both cone sheaths and OS are smaller in regions of high receptor density and larger at the periphery (compare Fig. 7C to 7A or 7H). Among these 8 micrograph pairs, S-cones appear to have the lowest density in the superior retina (Fig. 7B,E,F) except for the far periphery (Fig. 7A) and the *area centralis* (Fig. 7C). In these latter two regions, however, the percentages of S-cones are vastly different. The relatively dense field of S-cones at the superior far periphery (Fig. 7A; 1,300/mm^2) represents over 27% of all cones in a region of relatively low total cone density (4,700/mm^2), whereas the localized increase in S-cones at the *area centralis* (1,000/mm^2) is swamped by the crowded field of total cones found there (19,000/mm^2) and contributes only 5.5% to this total num-

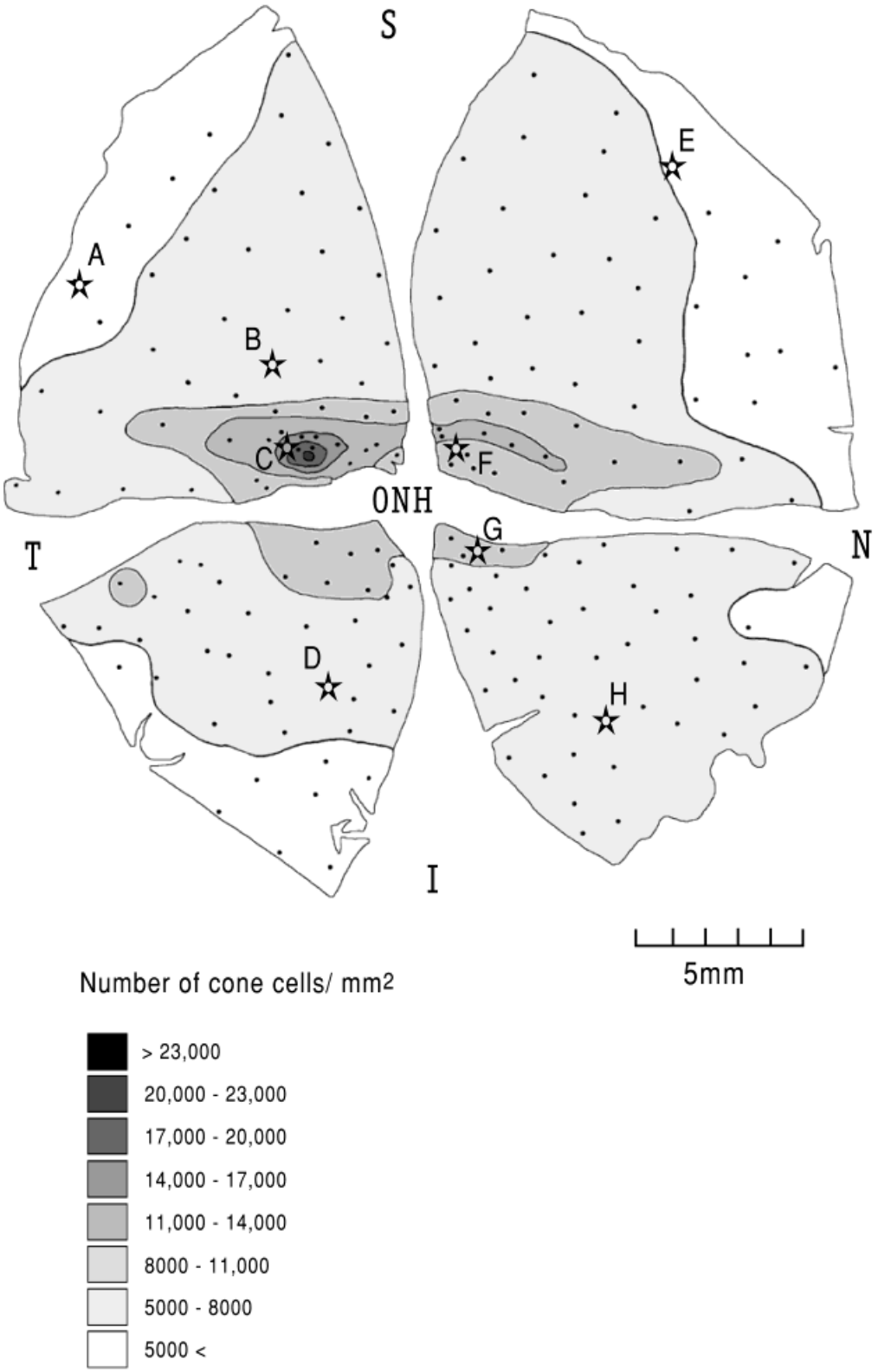

Fig. 6. Schematic diagram of cone distribution in a wholemounted cat retina (left eye; photoreceptors face up) depicting regional variations in cone density (see gray scale, bottom left). One hundred ninety-five areas of approximately 0.2 mm^2 each were sampled (black dots), accounting for 252,006 cones. Peak cone density lies at the *area centralis* within an elongated region of higher cone density along the nasotemporal axis. Cone populations at sites A–H are pictured in Figure 7. ONH, optic nerve head; S, superior; T, temporal; N, nasal; I, inferior.

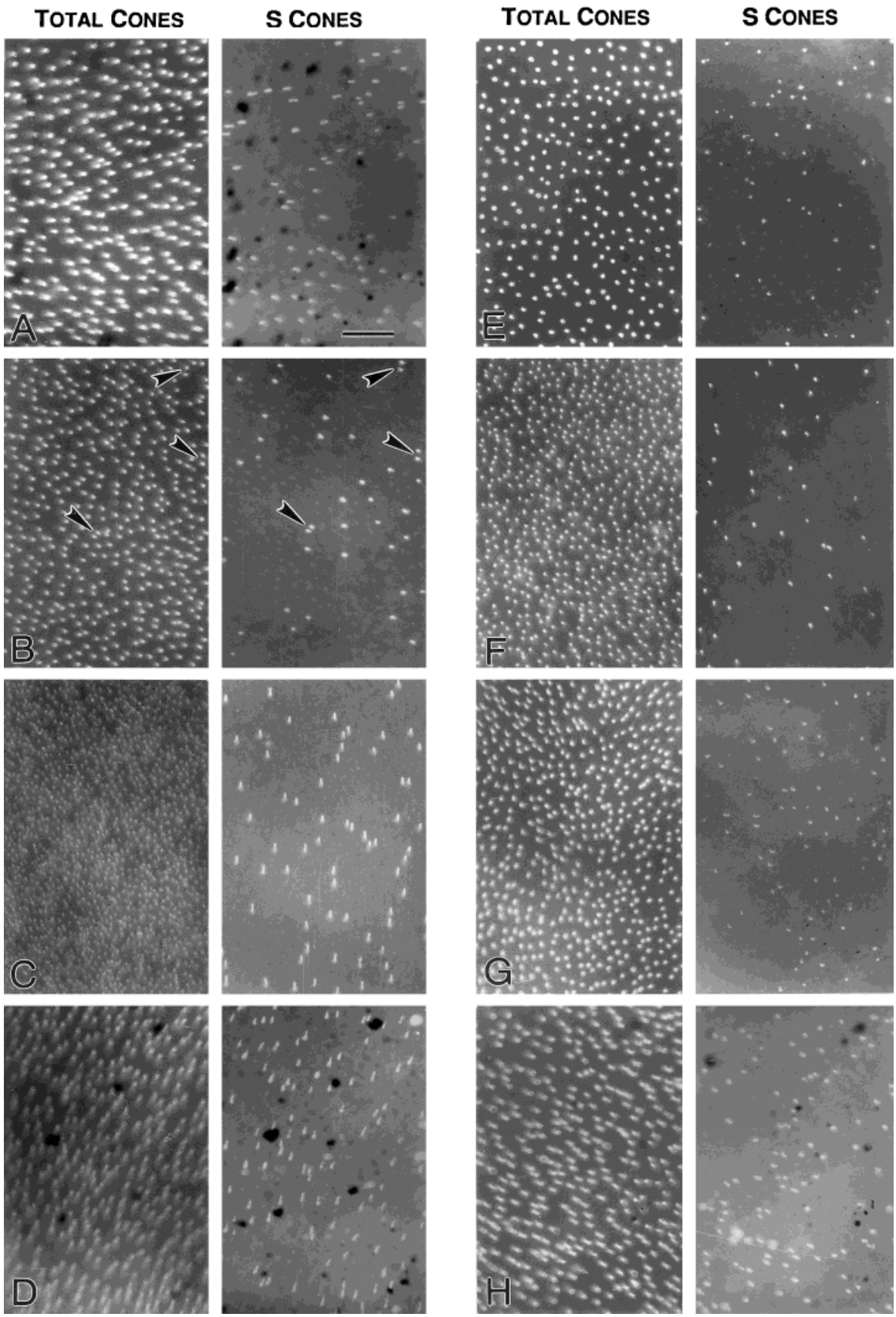

Figure 7

ber. S-cones achieve their highest densities in the inferior midperiphery (Fig. 7D; 1,900/mm^2) and across the inferior retina in general (Fig. 7G,H). Note that S-cones do not form a regular geometrical array at any of these retinal eccentricities.

Because we found no evidence for PNA-positive sheaths around rods, the M-cone density at any given location should represent the difference between the total cone and S-cone densities. We generated such differential data for the 180 sample sites (black dots, Fig. 8A) in a second retina (depicted on the right in Fig. 5), whose distribution of total cone density is shown by Figure 8A, the pattern of which is virtually the same as that shown in Figure 6. Because M-cones predominate in the cat's retina, the isodensity map for these cones (Fig. 8B) closely resembles that for total cones (Fig. 8A). A central peak of 26,000 M-cones/mm^2 falls to only 2,200/mm^2 at the inferior far periphery. The gray scales for Figure 8A and 8B are the same. A very different pattern of cone density emerges for the S-cones (Fig. 8C). Note that the gray scale covers a range less than one-tenth of that in Figures 6, 8A, and 8B. Peak S-cone densities of over 1,500/mm^2 lie at the far periphery, at the *area centralis* itself, and across the center of the inferior hemiretina. Lowest S-cone densities between 500 and 600/mm^2 occur in a broad region across the superior retina outside the *area centralis*. The local increase in S-cone density centrally vanishes when percent S-cones is charted (Fig. 8D). S-cones make up 12.9% of the total cones in this retina, averaging 9.8% in the superior retina and 16.4% of the inferior retina. S-cones comprise nearly 1 out of every 3 cones at the far retinal margins where such a high percentage results from a local peak in S-cone density coupled with a trough in M-cone density. A similar high S-cone density at the *area centralis* is all but hidden by the localized peak of M-cones resulting in a low S-cone density (5.5%) typical for most of the central superior retina. The broadest expanse of high S-cone density spans the central portions of the inferior hemiretina.

Fig. 7. A–H: Micrographs of 8 sampled areas corresponding to sites labeled A–H in Figure 6. Each pair consists of the same region showing total cones (peanut agglutinin [PNA] labeling, left photograph) versus short wavelength (S)-cones (anti-S opsin, right photograph). S-cones do not form a recognizable regular array at any retinal eccentricity. **A:** At the far superior periphery, a high S-cone density (1,300/mm^2) and a low total cone density (4,700/mm^2) yields a narrow region where S-cones comprise 27.1% of the cone population. Dark blotches in this and other peripheral regions are small patches of adherent retinal pigmented epithelial (RPE) cells. **B:** The superior midperipheral retina typically contains a broad region of low S-cone density (500/mm^2; right) comprising only 7.7% of the total cone population (6,900/mm^2). Several closely spaced S-cones are indicated by arrowheads for purposes of comparison. **C:** At the edge of the *area centralis*, a localized increase in S-cone population (1,000/mm^2) is eclipsed by the peak in total cone population (19,000/mm^2) such that S-cones only constitute 5.5% at this site. **D:** S-cones have their highest density (1,900/mm^2) and relative percentage (31.9%) in the inferior midperiphery where total cones only number 6,000/mm^2. **E:** At a site in the superior periphery farther from the ora serrata than in A, S-cone density (900/mm^2) and percentage (20.1%) are elevated over more central regions. Total cones number only 4,600/mm^2. **F:** In the pericentral superior retina, S-cones (800/mm^2) constitute only 7.0% of the total cone density (10,500/mm^2). **G:** In the inferior midperiphery, total cone density has fallen off (8,400/mm^2), whereas the S-cone population has risen (1,200/mm^2; 13.9%). **H:** At the inferior periphery, the lowest total cone density encountered (5,700/mm^2) coupled with a high S-cone density (1,800/mm^2), results in their comprising 31.0% of total cones at this site. Scale bar in A = 50 μm (applies to all panels).

Detached cat retina

Labeling with PNA and antibodies against S-cone opsin and calbindin D. In the second phase of our study, we initially planned to use the same markers that we used on normal tissue to quantify the number and types of cone at 1, 3, 7, and 28 days after experimental retinal detachment. Early in our investigation, it became clear that the PNA-positive sheaths around cones disappear rapidly (Rex et al., 1997) and thus could not be used reliably to quantify the numbers of cone photoreceptors present at timepoints of 3 days postdetachment and beyond. In this same study using antibodies against both cone opsins, the amount of labeling by each also decreased dramatically at 3 days and beyond. The antibody to calbindin D was selected as a more reliable marker after detachment than either PNA or the opsins. This probe is known to robustly label entire cones from their OS to their terminals (Schreiner et al., 1985; Pasteels et al.,, 1990; Figure 3 shows a transverse section of normal cat retina labeled with the antibodies against M/L-cone opsin and calbindin D. The latter antibody stains the entire cell; the former colocalizes in the OS of all but the S-cones). We first double-labeled wholemounts of normal retina with the lectin PNA and the antibody against calbindin D to assess whether the latter gave a total cone population similar to that labeled by the lectin. Calbindin D in normal retina gave cone densities that corresponded closely to those obtained by PNA labeling (Fig. 9, top; Table 1) except near the *area centralis* where we noticed an unexpected phenomenon. Whereas most cones across the retina have calbindin D-positive OS surrounded by PNA-positive cone sheaths (Fig. 4a), a majority of cones within the *area centralis* fail to label with the antibody to calbindin D (Fig. 4b). This observation invokes studies in monkey (Röhrenbeck et al., 1989; Pasteels et al., 1990) and human retina (Haley et al., 1995) showing that foveal cones fail to label with antibodies to calbindin D. Except for this most central region, the data on the overall cone population were very similar whether the labeling was by PNA or the calbindin D antibody (see below). In preliminary studies, the anti-calbindin D labeling seemed to persist longer than that with the antibodies to cone opsins; thus, we felt encouraged to use this cone marker in our detachment series.

Quantitative analysis of cone distributions in the detached cat's retina. To first determine whether anti-calbindin D labeling yields similar data as the lectin PNA, a normal, superior temporal (ST) quadrant (containing the *area centralis*) was labeled with this antibody along with one directed to S-cone opsin. Thirty-five sites were studied covering a total of 6.3 mm^2 containing 54,719 calbindin-positive cells and 4,948 S opsin-positive cones, or only 9.0% (see Table 1). Compared to the bright fluorescence of the PNA-positive sheaths, the calbindin D antibody labeled less intensely and was by far the more difficult to photograph (Fig. 10A, left). Nevertheless, the isodensity maps of anti-calbindin D-positive cells for the ST quadrant (Fig. 9, NORMAL, left) closely resemble the maps of the same quadrant in the normal eyes shown in Figures 6 and 8A, with the notable exception of the *area centralis*, where the peak density (19,700/mm^2) is about 25% lower, reflecting the failure of calbindin D to stain

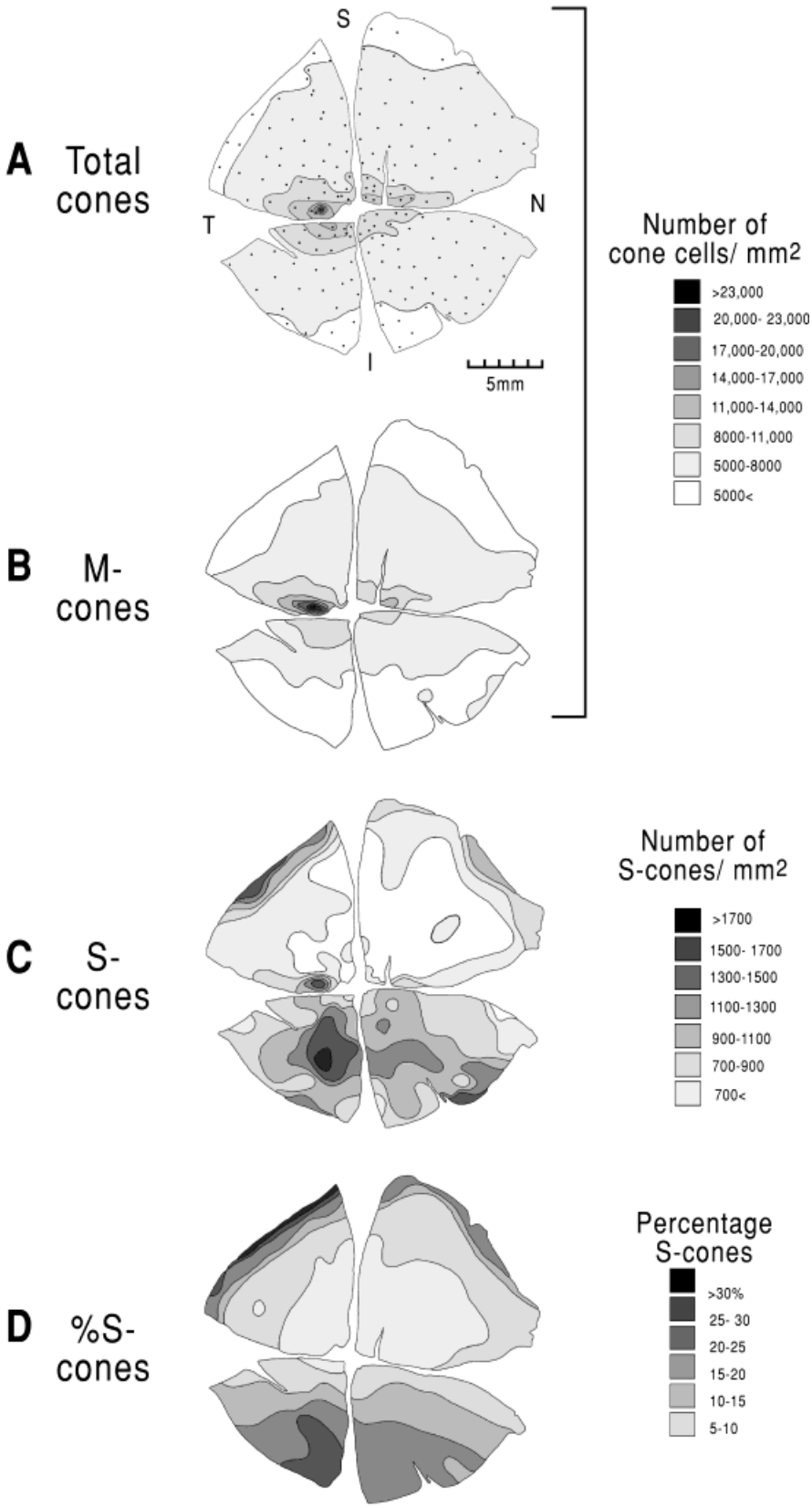
A Total cones
S
T
N
I
5mm
Number of cone cells/ mm2
>23,000
20,000- 23,000
17,000-20,000
14,000-17,000
11,000-14,000
8000-11,000
5000-8000
5000<
B M- cones
C S- cones
Number of S-cones/ mm2
>1700
1500- 1700
1300-1500
1100-1300
900-1100
700-900
700<
D %S- cones
Percentage S-cones
>30%
25- 30
20-25
15-20
10-15
5-10

Figure 8

many of the cones in this central region as described above (see Fig. 4b). Thus, calbindin D proved a reliable cone marker in the wholemounted controls. The isodensity map for S-cones (Fig. 9, NORMAL, right) looks more complex than that for the ST quadrant in Figure 8C because its gray scale is more finely divided; yet there remains a localized density peak at the *area centralis* and higher densities at the far periphery. Most S-cone densities outside the *area centralis* fall between 500 and 800/mm^2.

From an experimental standpoint, two problems immediately arose when switching from normal to detached tissue. After detachment, the uniform apposition of retina and RPE is gone and the detached retina "floats" in the vitreous freely albeit unevenly above the RPE. These detached retinas move easily, not always lying directly over their previous sites. Such positional uncertainty makes comparisons with specific locations in normal retinas largely approximations. This problem is compounded by the tendency of the surface of the detached retinas to wrinkle. This wrinkling worsens across the first week postdetachment, but was less of a problem by 28 days postdetachment, at which time the retina itself is much thinner. Despite these difficulties, we tried to use retinal landmarks—the optic nerve head, major blood vessels, and the *area centralis* particularly—to estimate retinal location in the detached tissue. In an attempt to limit the number of experimental animals, we did not stain any experimentally detached wholemounts with the JH492 antibody to M/L-cone opsins. Although previous studies indicate a reduction in M/L-opsin expression after retinal detachment (Rex et al., 1997) we offer here no quantification of M-cones after detachment.

After a single day of detachment, both antibodies still stain quite robustly, although the calbindin D-positive cells display greater variations in diameter and in staining intensities (Fig. 10B, left) than in the normal retina. We noticed that although most cones lay in a single plane of focus as occurs in the normal retina, a minority of cells lay somewhat deeper in the outer nuclear layer. S opsin-positive profiles after detachment show a greater range of diameter and shape (Fig. 10B, right) than normal (Fig. 10A, right). An *area centralis* is still evident by using either antibody (Fig. 9, 1d RD; note: only the cats' right eyes are used for the detachments; hence, the labeling patterns in the experimental eyes are mirror images to those in the controls; e.g., Figs. 6, 8A. In Figure 9, we flipped the data for the normal left eye 180° to facilitate its comparison to the detached retinas from the experimentally detached right eyes). Thirty-six sample sites measuring a total of 4.8 mm^2 were studied that contained 16,554 calbindin D-positive profiles and 2,190 S opsin-positive profiles, or 13.2% of total cones (see Table 1), assuming that all of the latter were included in the former, which seems not to be the case. In doubled-labeled wholemounts of detached retina, we noted that as early as 1 day after detachment, a minority of cones whose OS were labeled by the S-opsin antibody failed to be stained by the calbindin D antibody in each of the sample areas. Calbindin D labeling proved to be increasingly problematic with longer detachment periods; at 28 days, only patches of cells were faintly labeled by this antibody. We are not certain whether this decline in labeling occurs uniformly in both cone types. It did not show any particular specificity to retinal regions, occurring in all of the areas examined. Nonetheless, after 1 day of detachment, those cones that still were labeled by calbindin D show the typical central to peripheral decrease in density of labeled cells (Fig. 9, 1d RD, left), but the absolute numbers centrally (9,000/mm^2) are roughly half that of normal eyes (see Fig. 9, NORMAL, left; Table 1). Most midperipheral densities ranged between 1,600 and 5,200/mm^2, but some far peripheral sites have as few as 600/mm^2. S-cone densities show dramatic decreases with most regions having densities between 300 and 500/mm^2. Nonetheless, there is still evidence of a central to peripheral gradient with this antibody as well (Fig. 9, 1d RD, right; Table 1). Many cones positive for anti-S opsin are calbindin D-negative, a phenomenon no longer restricted to the *area centralis*.

The 3-day detached retinas were so wrinkled that it was often impossible to find regions near the selected sample sites with large enough expanses of tissue lying in the same plane of focus to fill our usual 0.2 mm^2 photographic field. In such instances, cell counts were made in carefully matched portions of these pre-selected fields. Thirty-six sample areas were surveyed that together covered 3.9 mm^2 of retina. In sum, we counted 21,043 calbindin D-positive cones and 1,743 S opsin-positive cones, or 8.3% of total cones (see Table 1). Instead of a strong central-to-peripheral gradient, the calbindin D labeling appeared more homogeneous with the central half of the quadrant containing 5,000 to 7,500 cones/mm^2, whereas the peripheral half contained somewhat fewer at 2,800 to 5,000/mm^2 (Fig. 9, 3d RD, left). Calbindin D labeling, though reduced in absolute density, appeared more uniform than at 1 day postdetachment (Fig. 10C, left). The S opsin-positive cones continue to decrease dramatically; the sparse profiles display a range of size and shape (Fig. 10C, right). Except for one small central region with over 300 labeled profiles/mm^2, most regions contain between 100 and 200/mm^2 (Fig. 9, 3d RD, right). The bands of higher S-cone density at the bottom of the quadrant represents a transitional region to the attached inferior retina with more normal levels of S-cone labeling.

Trends described above for the 3-day detached retina continue to be seen in the 7-day detached retinal quadrant which is even more wrinkled (Fig. 10D, left), further hindering systematic sampling. Calbindin D labeling contin-

Fig. 8. Schematic diagrams of cone distributions in a retinal wholemount of normal cat #2 of Figure 5. **A:** Total cone density. Peanut agglutinin (PNA) lectin was used to stain cone matrix sheaths; anti-S opsin to label short wavelength (S)-cone outer segments (OS). One hundred eighty areas were sampled (black dots), accounting for 226,784 cones. A sharp peak of just under 28,000 cones/mm^2 was counted at the *area centralis*. Cone densities declined rapidly away from this central region, though more slowly along the horizontal nasotemporal axis wherein a smear of higher density is found. One site at the far inferior periphery had the lowest total cone density of 3,100/mm^2. **B:** Medium wavelength (M)-cone density. Because M-cones predominate in the cat's retina, the isodensity map for M-cones closely parallels that of total cones (compare with Figs. 6, 8A). **C:** S-cone density. The robust fluorescence of labeled S-cone outer segments facilitated density counts. Peak S-cone densities lie at the far periphery, at the *area centralis* itself, and in the central portions of the inferior hemiretina. Lowest S-cone densities occur in a broad region across the superior retina outside the *area centralis*. **D:** Percent S-cones. A low S-cone percentage is typical for most of the central superior retina, whereas a broad expanse of the inferior hemiretina contains the highest S-cone percentages. S, superior; T, temporal; N, nasal; I, inferior.

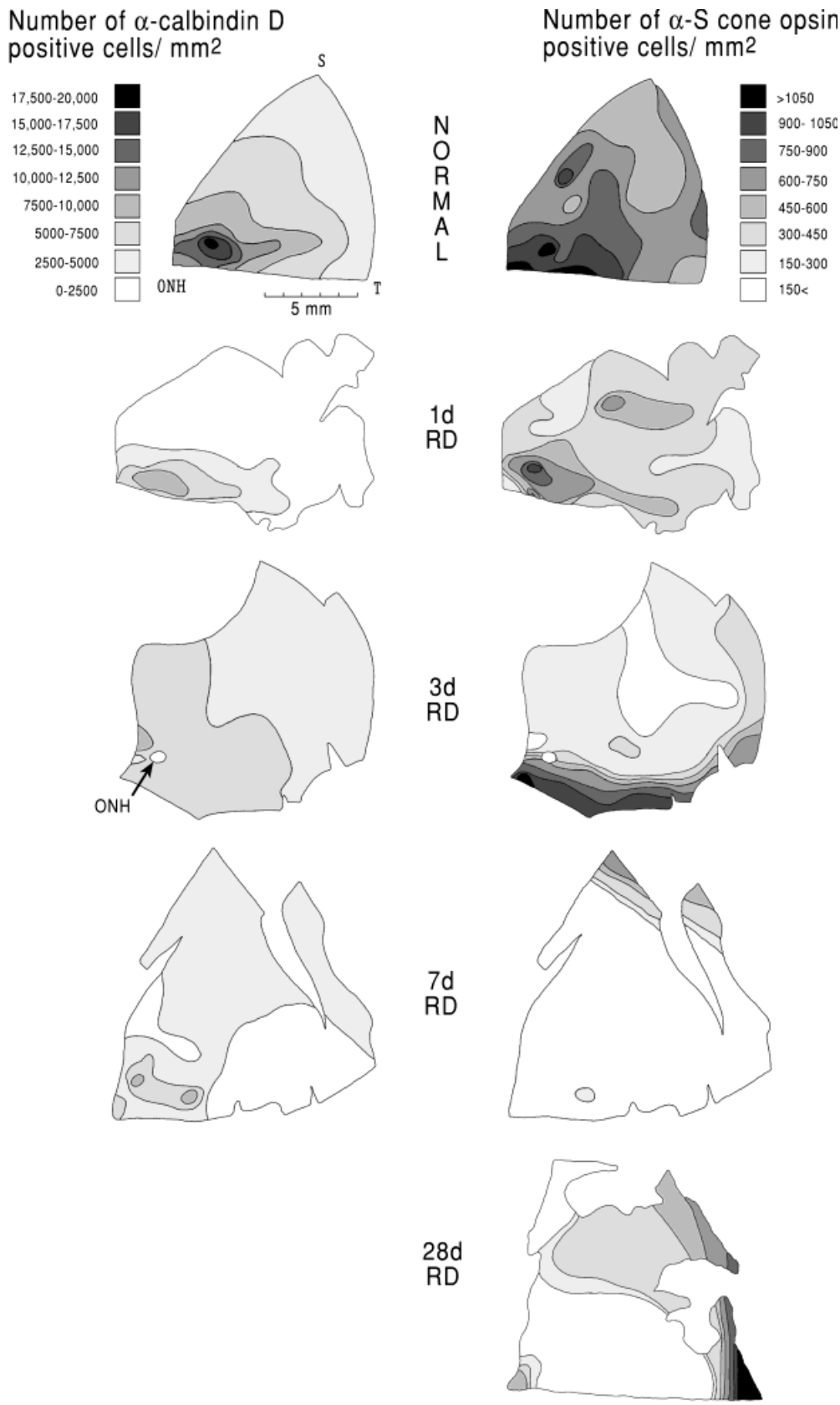
Number of α-calbindin D positive cells/ mm2
17,500-20,000
15,000-17,500
12,500-15,000
10,000-12,500
7500-10,000
5000-7500
2500-5000
0-2500
S
ONH
T
5 mm
Number of α-S cone opsin positive cells/ mm2
>1050
900- 1050
750-900
600-750
450-600
300-450
150-300
150<
NORMAL
1d RD
3d RD
7d RD
28d RD
ONH

Figure 9

TABLE 1. Counts and Densities of Photoreceptors Labeled With Antibodies to Calbindin D and S-Cone Opsin

Experimental condition	Sample area (mm^2)	Total number of positive cells counted in sample area		Density of cells/mm^2					
				Retina			Retina		
				Central	Mid	Peripheral	Central	Mid	Peripheral
		Calbindin D	S-Opsin	Calbindin D			S-Opsin		
Control	6.3	54,800	4,950	19,700	7,000	2,800	1,100	1,100	800
1-day detached	4.8	16,600	2,200	9,000	5,200	1,700	700	500	400
3-day detached	3.9	21,000	1,700	7,300	3,900	2,800	400	200	100
7-day detached	3.8	11,600	300	8,000	3,600	1,500	200	30	30
28-day detached	5.6	—	900	—	—	—	200	40	40

ues to decrease, showing an inconsistent distribution within the various sample areas, some being uniform across the field (Fig. 10D, left), whereas others are not. Peak densities of over 8,000 profiles/mm^2 are restricted to two small central regions; densities of 5,000 to 7,500/mm^2 encircle these. Densities of 2,500 to 5,000/mm^2 cover most of the quadrant with densities under 2,000 and as low as 300/mm^2 restricted to two mid-peripheral regions (see Fig. 9, 7d RD, left; Table 1). Forty-three sample sites, together comprising 3.8 mm^2 of retina, yielded 11,603 calbindin D-positive cells and only 304 S opsin-positive profiles (2.6%; see Table 1). At each sample area, S opsin-positive OS are even scarcer than at 3 days postdetachment. Only one central site had S opsin-positive profiles exceeding 250/mm^2, whereas many sample sites had only one or two profiles (Fig. 10D, right) representing densities of under 100/mm^2, with several regions having no positive profiles whatsoever. As a result, only the far periphery of the ST quadrant had elevated numbers of S opsin-positive OS, perhaps reflecting their proximity to attached peripheral retina.

After 28 days of detachment, the wholemount of the ST quadrant was thin and had far fewer wrinkles, permitting easier sampling. Thirty-six sites totaling 5.6 mm^2 were surveyed (see Table 1). Labeling with anti-calbindin D was spotty and sufficiently weak to prohibit effective data collection. OS labeled with anti-S opsin, though rare, still stained brightly and 889 S opsin-positive profiles of varying size and shape were counted. Many of these profiles, however, were localized to superior peripheral regions (Fig. 9, 28d RD) whose higher densities, relative to the 3- and 7-day detachments, may reflect this region's reapposition to the RPE. The broad central portion of the quadrant continued to show decreasing densities of S-cones, many sample areas having densities between 20 and 50/mm^2 which were between 5% and 10% of normal levels of labeling.

Table 1 shows a summary of the data collected from this series of wholemounts. It shows the decline in the total numbers of cones labeled with either the calbindin D or S-opsin antibodies as well as the decline in density for each of these markers in broad zones of retinal eccentricity. Whether the M-cones show a similar decline in numbers remains unknown, although data from Rex et al. (1997) would suggest a similar phenomenon.

Fig. 9. Anti-calbindin D (left column) and anti-S cone opsin (right column) labeling in normal and detached superior temporal quadrants. Differing gray scales to the right and left apply to the underlying columns. S, superior periphery; T, temporal periphery, ONH, optic nerve head. Control eye (NORMAL): A superior temporal quadrant stained with anti-calbindin D (left) and anti-S cone opsin (right). An isodensity map closely resembles the map for total cones derived from PNA staining (Figs. 6 and 8A) except in the *area centralis* (see text). The isodensity map for S-cones is similar to the superior temporal quadrant of the wholemount in Figure 8C but a different gray scale is used in order to allow comparison with the detached retinas below. One day retinal detachment (1d RD): Left, calbindin D-labeled cones show the typical central to peripheral decrease in density of labeled cells, but the absolute numbers centrally are roughly half that of normal eyes (see Fig. 7A). Peripheral densities have also dropped. Right, S-cone densities show a dramatic decrease (see text). Three day retinal detachment (3d RD): Left, the density of calbindin D-positive cone labeling continues to decrease; the isodensity map appears more homogeneous. Right, S-cone labeling has been reduced to less than half normal levels. Only a slightly elevated S-cone density marks the region of the *area centralis*. The peripheral and inferior borders showing more normal levels of S-cone labeling represent zones of transition to regions of attached retina. Seven day retinal detachment (7d RD): Left, except for a region near the *area centralis*, most of the detached retina has levels of calbindin D labeling less than the lowest observed in normal retina. Right, S-cone labeling in the detached region has fallen to about 20% of normal. Twenty-eight day retinal detachment (28d RD): Right, S-cone labeling has been reduced to 5% to 10% of normal with no remaining evidence of the S-cone peak near the former *area centralis*.

DISCUSSION

Cats are renowned for their scotopic vision. Their retinas contain mostly rod photoreceptors whose number and distribution have been carefully detailed (Steinberg et al., 1973). In this same study, Steinberg et al. (1973) reported the overall distribution of cones, though they could not distinguish between spectral subtypes. Since that time, antibodies have been developed that can specifically label the short wavelength-sensitive (S-) versus the middle-to-long wavelength-sensitive (M/L-) cones. Even though the JH492 antibody used here cannot distinguish between the M- and L-cone opsins (Wang et al., 1992), that limitation is not a concern in cat because the feline retina lacks L-cones (see Jacobs, 1993). The relative distributions of S- and M-cones in cat retina were unreported until now.

Although the first morphological identification of S-cones in the overall mosaic of photoreceptors was accomplished by using Procion yellow (DeMonasterio et al., 1981), the development of monoclonal antibodies specific to the two spectral types of cone by Szél et al. (1985, 1988), was the breakthrough necessary to start systematic surveys of cone populations in various vertebrate species. Taken together, these studies have revealed two patterns of association of the two cone types: homogeneous and heterogeneous (Szél et al., 1996). In the former, both spectral subtypes are found at all points on the retinal surface, whereas in the latter, certain broad regions of the retina contain only S-cones. In mammalian retinas, the former

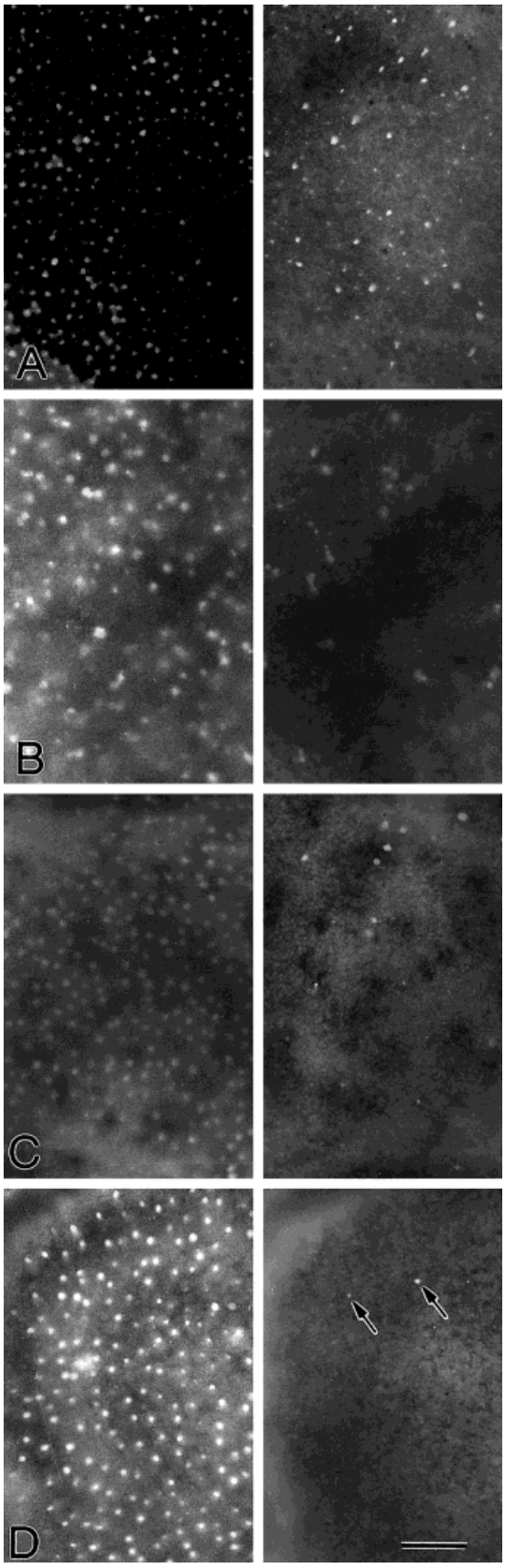

pattern with M-cones vastly outnumbering S-cones is the norm (Szél et al., 1996), whether the retina contains less than 1% (rat; Szél and Röhlich, 1992) or over 80% cones (ground squirrel, Long and Fisher, 1983; Ahnelt, 1985; Szél and Röhlich, 1988; Kryger et al., 1998). Within the broad confines of these patterns, most mammalian species have various topographic regions of heightened cone density (fovea, *area centralis*, visual streak) to subserve high acuity vision. Hughes (1977) has associated fovea- and *area centralis*-containing retinas to arboreal species, whereas those retinas with visual streaks were linked to species living on the field, plain, or veldt. Many species have varying combinations of these two patterns, including the cat with its *area centralis* and a broad horizontal smear of high cone (Steinberg et al., 1973) and ganglion cell (Stone, 1965; Hughes, 1975) density.

The ability to label all cones with PNA, and either subset of cones with a specific antibody, allowed us to determine the relative populations of each cone type. The absolute cone densities described here are in close agreement with those reported by Steinberg et al. (1973). Not only did we find similar peak cone densities at the center of the *area centralis*, but similar decreases in cone density with increasing eccentricity, and a broad horizontal region of high cone density that is larger temporally than nasally. We have also extended the data on cone density into the far superior and inferior regions of the retina beyond the regions described by Steinberg et al. (1973). Because M-cones comprise 83% to 88% of total cones, it should not be surprising that this spectral class has a distribution similar to and underlying that of the total cone population. The S-cones have a very different topographical pattern, with the broadest region of S-cone density occurring across the central inferior retina, the nontapetal region of the globe. Elevated S-cone densities have been described in the ventral retina of house mice (Szél et al., 1992; Wang et al., 1992) and rabbits (Juliusson et al., 1994). Unlike the cat, however, these particular species have heterogeneous cone distributions. The S-cones are the only cone type found across the entire inferior retina of the house mouse, and are the only cone type in the inferior periphery of the

Fig. 10. Calbindin D (left column) and S-cone labeling (right column) in normal (A) and detached (B–D) retinas. **A:** Normal retina. A uniform field of calbindin D-labeled cones shows the variation of staining intensity typical for this antibody. Most cells are of similar diameter; their density at this location just under 6 mm of eccentricity is 5,800/mm^2. S-cone density for this same area is just under 500/mm^2. Many of these labeled cells can be identified as some of the more brightly calbindin D-positives cells to the left. **B:** After 1 day of detachment, the calbindin D-positive profiles display a wide range of size and staining intensity. Many profiles lie at a slightly deeper plane of focus than that photographed here, about 3 mm of eccentricity. Calbindin D profiles have a density of 2,200/mm^2. S-cone density at this same location is just over 400/mm^2. The labeled profiles assume the widest range of size and shape at this timepoint. **C:** At 3 days after detachment, calbindin D labeling is erratic. Here a relatively uniform field of calbindin D-positive profiles has a density of 4,200/mm^2 and lies about 7 mm from the presumed *area centralis*. Note the wrinkling of the retina as it leaves the plane of section at the top and bottom of the figure. S-cone labeling is spotty, here just under 140/mm^2. **D:** At 7 days after detachment, a relatively uniform field of calbindin D-positive cells lies on the edge of a retinal fold at about 6 mm of eccentricity. The cell density here is just over 4,100/mm^2. Only 2 short wavelength (S)-cones are labeled (arrows) representing a density of only 32/mm^2. Scale bar = 50 μm.

rabbit retina where they form the so-called "blue streak" (Juliusson et al., 1994). The retina of the cat differs from these two species because its S-cone- rich region still contains a majority of M-cones. S-cone densities are lowest across most of the superior cat retina with two notable exceptions. Unexpectedly, one of the highest S-cone densities in the cat retina, over 30% of total cones, occurred in a very narrow band at the far superior-temporal periphery, a phenomenon similar to a narrow region of high S-cone density reported in the far superior-nasal periphery in the California ground squirrel retina (Kryger et al., 1998). More significantly, there is a localized peak of S-cone density in the *area centralis* itself which departs from the pattern in the foveae of adult humans and other diurnal primates where S-cones are lacking or are very few (DeMonasterio et al., 1985; Szél et al., 1988; Wikler and Rakic, 1990; Curcio et al., 1991; Bumsted and Hendrickson, 1999; Martin and Grünert, 1999).

A major rationale for undertaking this study was to gain quantitative information about the fate of cones after retinal detachment. It is common knowledge that foveal detachments are at high risk for severe loss of vision, and that altered color vision is one of the significant changes in vision reported after retinal reattachment (Nork et al., 1995). Thus, additional knowledge about the survival capacity of cone photoreceptors is particularly relevant. Importantly, in human detachments there is some evidence based on studies of carbonic anhydrase cytochemistry that the S-cones are much more sensitive to damage than the M-cones (Nork et al., 1995). Indeed, in that report, it was concluded that *all* of the S-cones were either lost or showed signs of what the authors termed "irreversible damage," within a few days of detachment. They also concluded that the M-cones lost carbonic anhydrase after detachment, thus complicating their ability to use the absence of that enzyme as a marker for the S-cones. That particular observation seems germane to our showing that all reliable markers that we have used for cones in normal retina (e.g., PNA, anti-opsins, anti-calbindin D; also see Rex et al., 1997) become highly unreliable markers after detachment as they rapidly decrease or even disappear from the cones. This fact made it difficult for us to determine unequivocally the fate of the cone population as a whole. It also made absolute conclusions tentative about the fragility of the S-cones relative to that of the M-cones, although our subjective impression is that they react more rapidly. Our results do indicate, though, that significant numbers of cones, including S-cones, survive in the animal model. The data from central retina (Table 1), show that at 1 day of detachment, the number of cones labeled with anti-calbindin D has dropped to 46% of that in control eyes, whereas the number of S opsin-labeled cones is at 64%. Interestingly, although the number of labeled cells seems to decline fairly rapidly for both markers, the further decline in the number of anti-calbindin D-labeled cells is then slight out to 7 days of detachment, whereas the number of anti-S opsin-labeled cells continues to drop to 18%. Because the calbindin D antibody presumably labels all cones (outside the center of the *area centralis*), the more rapid loss of anti-S-cone labeling probably does reflect their relatively greater reactivity to injury. Although the anti-calbindin D labeling was too faint at 28 days to allow accurate counting of the labeled cones, it had not completely disappeared from these cells. Indeed, our impression was that the overall density of cones labeled by calbindin D was about the same as at 7 days. Certainly we know that some cones die after detachment because they label by the TUNEL (TdT-mediated duTP-biotin nick end labeling) technique, which detects apoptotic cells (data not shown). What we cannot confirm is that nearly all of the S-cones die as concluded by Nork et al. (1995) in humans. Perhaps the cells that they identified as "irreversibly damaged," based on structural criteria, were indeed not fated to certain death. Rather, those cells may have survived, but with a highly altered morphology reflecting adaptive mechanisms involving, for example, a rapid decline in the expression of specific protein molecules, and/or a loss of mitochondria (Mervin et al., 1999).

It would seem at this point that a more decisive answer to the question of cone survival could be obtained by simply counting cone cells by using counterstained, semithin sections or unstained wholemounts as done by Steinberg et al. (1973). In the normal retina, cone cell bodies are easily recognized because they lie in a single row near the outer limiting membrane, and have larger inner segments and cell bodies than the adjacent rods. Unfortunately, after detachment it is quite apparent that the cell bodies of surviving cones often shift their location, moving deeper into the ONL, and that they lose much of their distinctive size and morphological differences from rods, making their identification difficult and unreliable (Erickson et al., 1983). Data from TUNEL labeling for apoptotic cells clearly show that some cones die (unpublished data), but determining exactly how many by that technique remains elusive because TUNEL labeling provides only a "snapshot" of the event, not a cumulative picture. We do have underway a series of experiments utilizing retinal reattachment that we believe will allow us to answer this important question. If, utilizing our various markers after surgical reattachment we find the number of cones to be significantly greater than the number identified with these markers at 3 or 7 days of detachment, then we will know that these cells obviously survived, because neurons are not thought to be generated in the adult mammalian retina, and thus any regeneration that occurs presumably would arise from pre-existing cells.

One outcome of this and other studies in our lab is the conclusion that cones react differently from rods after detachment. Unlike cones, surviving rods continue to express every protein that we have investigated by immunocytochemistry, indeed, even increasing their expression of some (e.g., phosducin; Fisher et al., 1996).

Regardless of the eventual details of the outcome, all of our data indicate that cone photoreceptors react profoundly to detachment. Understanding their reaction to injury, and their differences from rods may lead to treatments that will either rescue cones from degeneration or promote their ability to regenerate (see Lewis et al., 1999; Mervin et al., 1999). This may be important in conditions other than retinal detachment, for example, age-related macular degeneration, the greatest cause of blindness in the industrial word in people over the age of 65, and a condition that preferentially affects the cone-rich macula.

ACKNOWLEDGMENTS

The authors acknowledge Maura Jess for her expertise in generating the computer-based illustrations as well as the technical assistance of Jonathan Kelling, Cherlin Johnson, and Peter John Kappel.

LITERATURE CITED

Ahnelt PK. 1985. Characterization of the color related receptor mosaic in the ground squirrel retina. Vision Res 25:1557–1567.

Anderson DH, Guérin CJ, Erickson PA, Stern WH, Fisher SK. 1986. Morphological recovery in the reattached retina. Invest Ophthalmol Vis Sci 27:168–183.

Blanks JC, Johnson LV. 1984. Specific binding of peanut lectin to a class of retinal photoreceptor cells. Invest Ophthalmol Vis Sci 25:546–557.

Bridges CDB. 1981. Lectin receptors of rods and cones. Visualization by fluorescent label. Invest Ophthalmol Vis Sci 20:8–16.

Bumsted K, Hendrickson A. 1999. Distribution and development of short-wavelength cones differ between Macaca monkey and human fovea. J Comp Neurol 403:502–516.

Cleland BG, Levick WR. 1974. Properties of rarely encountered types of ganglion cells in the cat's retina and an overall classification. J Physiol 240:457–492.

Cook B, Lewis GP, Fisher SK, Adler R. 1995. Apoptotic photoreceptor degeneration in experimental retinal detachment. Invest Ophthalmol Vis Sci 36:990–996.

Curcio CA, Allen KA, Sloan KR, Lerea CL, Hurley JB, Klock IB, Milam AH. 1991. Distribution and morphology of human cone photoreceptors stained with anti-blue opsin. J Comp Neurol 312:610–624.

Daw NW, Pearlman AL. 1970. Cat colour vision: evidence for more than one cone process. J Physiol 211:125–137.

DeMonasterio FM, Schein SJ, McCrane EP. 1981. Staining of blue-sensitive cones of the macaque retina by a fluorescent dye. Science 213:1278–1281.

DeMonasterio FM, McCrane EP, Newlander JK, Schein SJ. 1985. Density profile of blue-sensitive cones along the horizontal meridian of macaque retina. Invest Ophthalmol Vis Sci 26:289–302.

Erickson PA, Fisher SK, Anderson DH, Stern WH, Borgula GA. 1983. Retinal detachment in the cat: the outer nuclear and outer plexiform layers. Invest Ophthalmol Vis Sci 24:927–942.

Fisher SK, Lewis GP, Lo G, Hussey RW, Fariss RN. 1996. Changes in the expression of photoreceptor specific proteins after experimental retinal detachment. Invest Ophthalmol Vis Sci 37:S1046.

Haley TL, Pochet R, Baizer L, Burton MD, Crabb JW, Parmentier M, Polans AS. 1995. Calbindin D-28k immunoreactivity of human cone cells varies with retinal position. Vis Neurosci 12:301–307.

Hughes A. 1975. A quantitative analysis of the cat retinal ganglion cell topography. J Comp Neurol 163:107–128.

Hughes A. 1977. The topography of vision in mammals of contrasting life style: comparative optics and retinal organization. In: Crescitelli F, editor. Handbook of sensory physiology, vol VII/5. Berlin: Springer Verlag. p 613–756.

Iwasaki M, Myers KM, Rayborn ME, Hollyfield JG. 1992. Interphotoreceptor matrix in the human retina: cone-like domains surround a small population of rod photoreceptors. J Comp Neurol 319:277–284.

Jacobs GH. 1993. The distribution and nature of colour vision among the mammals. Biol Rev 68:314–471.

Johnson LV, Hageman GS, Blanks JC. 1986. Interphotoreceptor matrix domains ensheath vertebrate cone photoreceptor cells. Invest Ophthalmol Vis Sci 27:129–135.

Juliusson B, Bergström A, Röhlich P, Ehinger B, van Veen T, Szél À. 1994. Complementary cone fields of the rabbit retina. Invest Ophthalmol Vis Sci 35:811–818.

Kryger Z, Galli-Resta L, Jacobs GH, Reese BE. 1998. The topography of rod and cone photoreceptors in the retina of the ground squirrel. Vis Neurosci 15:685–691.

Lewis GP, Linberg KA, Geller SF, Guérin CJ, Fisher SK. 1999. Effects of the neurotrophin brain-derived neurotrophic factor in an experimental model of retinal detachment. Invest Ophthalmol Vis Sci 40:1530–1544.

Linberg KA, Shaaw CL, Rex TS, Lewis GP, Fisher SK. 1998. The distribution of S and L cones in cat retina before and after retinal detachment. Invest Ophthalmol Vis Sci 39:S1059.

Long KO, Fisher SK. 1983. The distributions of photoreceptors and ganglion cells in the California ground squirrel, *Spermophilus beecheyi*. J Comp Neurol 221:329–340.

Loop MS, Millican CL, Thomas SR. 1987. Photopic spectral sensitivity of the cat. J Physiol 382:537–553.

Martin PR, Grünert U. 1999. Analysis of the short wavelength-sensitive ("blue") cone mosaic in the primate retina: comparison of new world and old world monkeys. J Comp Neurol 406:1–14.

Mervin K, Valter K, Maslim J, Lewis G, Fisher S, Stone J. 1999. Limiting photoreceptor death and deconstruction during experimental retinal detachment:the value of oxygen supplementation. Am J Ophthalmol 128:155–164.

Nork TM, Millecchia LL, Stickland BD, Linberg JV, Chao G. 1995. Selective loss of blue cones and rods in human retinal detachment. Arch Ophthalmol 113:1066–1073.

Østerberg, G. 1935. Topography of the layer of rods and cones in the human retina. Acta Ophthalmologica 6:1–103.

Pasteels B, Rogers J, Blachier F, Pochet R. 1990. Calbindin and calretinin localization in retina from different species. Vis Neurosci 5:1–16.

Rabin AR, Mehaffey L III, Berson EL. 1976. Blue cone function in the retina of the cat. Vision Res 16:799–801.

Rex TS, Lewis GP, Fisher SK. 1997. Rapid loss of blue and red/green cone opsin immunolabeling following experimental retinal detachment. Invest Ophthalmol Vis Sci 38:S35.

Ringo J, Wolbarsht ML, Wagner HG, Crocker R, Amthor F. 1977. Trichromatic vision in the cat. Science 198:753–755.

Röhrenbeck J, Wässle H, Boycott BB. 1989. Horizontal cells in the monkey retina: immunocytochemical staining with antibodies against calcium binding proteins. Eur J Neurosci 1:407–420.

Schreiner DS, Jande SS, Lawson DEM. 1985. Target cells of vitamin D in the vertebrate retina. Acta Anat 121:153–162.

Steinberg RH, Reid M, Lacy PL. 1973. The distribution of rods and cones in the retina of the cat (*Felis domesticus*). J Comp Neurol 148:229–248.

Stone J. 1965. A quantitative analysis of the distribution of ganglion cells in the cat's retina. J Comp Neurol 124:337–352.

Szél À, Röhlich P. 1988. Four photoreceptor types in the ground squirrel retina as evidenced by immunocytochemistry. Vision Res 28:1297–1302.

Szél À, Röhlich P. 1992. Two cone types of the rat retina detected by anti-visual pigment antibodies. Exp Eye Res 55:47–52.

Szél À, Diamantstein T, Röhlich P. 1988. Identification of the blue-sensitive cones in the mammalian retina by anti-visual pigment antibody. J Comp Neurol 273:593–602.

Szél À, Röhlich P, Caffé AR, van Veen T. 1996. Distribution of cone photoreceptors in the mammalian retina. Microsc Res Techn 35:445–462.

Szél À, Takács L, Monostori É, Vigh-Teichmann I, Röhlich P. 1985. Heterogeneity of chicken photoreceptors as defined by hybridoma supernatants. An immunocytochemical study. Cell Tiss Res 240:735–741.

Szél À, Röhlich P, Caffé, AR, Juliusson B, Aguirre G, van Veen T. 1992. Unique topographic separation of two spectral classes of cones in the mouse retina. J Comp Neurol 325:327–342.

Wang Y, Macke JP, Merbs SL, Zack DJ, Klaunberg B, Bennett J, Gearhart J, Nathans J. 1992. A locus control region adjacent to the human red and green visual pigment genes. Neuron 9:429–440.

Weinrich M, Zrenner E. 1983. Colour-opponent mechanisms in cat retinal ganglion cells. In: Mollon JD, Sharpe LT, editors. Colour vision: physiology and psychophysics. London: Academic Press. p 183–194.

Wikler KC, Rakic P. 1990. Distribution of photoreceptor subtypes in the retina of diurnal and nocturnal primates. J Neurosci 10:3390–3401.

Zrenner E, Gouras P. 1979. Blue-sensitive cones of the cat produce a rodlike electroretinogram. Invest Ophthalmol Vis Sci 18:1076–1081.